Università degli studi di Padova

Dipartimento di Fisica e Astronomia "Galileo Galilei"

Corso di Laurea in Fisica

Tesi di Laurea

Curvature effect on patterning dynamics on spherical membranes

Candidato: Leonardo Pacciani

Relatore: Prof. Enzo Orlandini

Anno accademico 2014-2015

To my family

Abstract

The aim of this thesis is to carry out an analytical study of the role that surface curvature may have on the evolution and selection of patterns seen as solutions of a set of reaction-diffusion equations defined on spheres. Such equations exhibit diffusion-driven instability of spatially uniform structures leading to spatially non-uniform textures such as coat markings of animals and pigmentation patterns on butterfly wings. While the case with planar domains has been thoroughly studied in the past, much less is known for reaction-diffusion equations defined on closed surfaces. Here we will consider the simpler case of spherical domains, and by describing the possible stationary solutions in terms of spherical harmonics, we will perform a linear stability analysis of the equations as a function of the radius R of the sphere (i.e. its curvature) and look for the most stable set of patterns compatible with that radius.

Preface

One of the most challenging questions in biology is the mechanism by which spatial patterns form in biological contexts; this process is called *spatial patterning*, and the underlying physical process is often modelled as the evolution of *reaction-diffusion systems*, namely chemical systems in which one or more reagents diffuse within a domain.
The study of how spatial patterns can form has many applications in a variety of biological fields, e.g. developmental biology, the dynamics of bacterial colonies, or behavioural aspects of territoriality in particular prey-predator systems. In particular, in developmental biology the properties of the mechanisms that involve the formation of spatial patterns have been used to describe the processes that lead to the formation of coat markings, or in general skin pigmentation, in animals, while in *morphogenesis* (a branch of embryology) they are a key concept in order to understand how an embryo can undergo cell differentiation and thus develop from a homogeneous spherically symmetric system to a complex organism. From this point of view, the study of spatial patterning on spherical surfaces is particularly relevant.
Even though the study of spatial patterning has shed light on different biological issues, many aspects of these processes are still not fully understood. For example, the mechanism that links genes and patterns, namely the way by which genetic information is physically translated into patterns and form during the development of an embryo, is one of those issues, although recent studies have given interesting hints on particular cases (see [3]).
It is thought that the formation of patterns occurs when the concentration of particular chemical substances, generally referred to as *morphogens*, exceeds a critical threshold level (*prepattern theory*). In other words, cells are thought to be "preprogrammed" to react to the morphogen concentration, and differentiate accordingly.
Thus, we can try to understand how such processes take place studying the spontaneous evolution of chemical reagents from a homogeneous to an inhomogeneous state; when this happen we say that the system exhibits *diffusion-driven instability*.
In particular, we say that a system exhibits diffusion-driven instability, or *Turing instability*, when its homogeneous steady state is linearly stable in the absence of diffusion, but becomes unstable to spatial perturbations when diffusion is present.

Contents

Chapter 1

Introductory study

In this part of the work we will lay out a general introductory study to determine the conditions for diffusion-driven instability for Gierer and Meinhardt's activator-inhibitor system, and we will determine its Turing space, i.e. the set of parameters within which it exhibits diffusion-driven instability.

1.1 Introduction

There are many possible reaction-diffusion systems, each one with its own experimental plausibility. In this work we will be concerned with a system composed of two chemical reagents, obeying Gierer and Meinhardt's activator-inhibitor equations. Namely, if $A(\vec{r},t)$ and $B(\vec{r},t)$ are the concentrations of the two compounds, which we call A and B, we have:

$$\frac{\partial A}{\partial t} = k_1 - k_2 A + k_3 \frac{A^2}{B} + D_A \nabla^2 A \qquad \frac{\partial B}{\partial t} = k_4 A^2 - k_5 B + D_B \nabla^2 B \,,$$

where $k_1, \ldots, k_5$ are (positive) constants and D_A, D_B are the diffusion coefficients of the two reagents.
In order to make these equations more easy to handle, we nondimensionalise them, by setting:

$$t^* = \frac{D_A}{L^2} t \,, \qquad \vec{x^*} = \frac{\vec{x}}{L} \,, \qquad \gamma = \frac{L^2}{D_A} k_5 \,, \qquad d = \frac{D_B}{D_A} \,,$$

$$a = \frac{k_1 k_4}{k_5^2} \,, \qquad b = \frac{k_2}{k_5} \,, \qquad c = \frac{k_3}{k_5} \,, \qquad u = \frac{k_4}{k_5} A \,, \qquad v = \frac{k_4}{k_5} B \,,$$

where L is a characteristic length of the system (e.g. the length of the domain if it is one-dimensional). In this way, we have (renaming t^* with t and $\vec{x^*}$ with $\vec{x}$):

$$\frac{\partial u}{\partial t} = \gamma \left(a - bu + c \frac{u^2}{v} \right) + \nabla^2 u \qquad \frac{\partial v}{\partial t} = \gamma (u^2 - v) + d \nabla^2 v \quad .$$

We have chosen to write these equations in this form because γ is a parameter with some useful interpretations, and in particular it is related to the size of the domain (i.e. L). As we shall see, this is crucial in order to understand how spatial patterning works on spherical surfaces.

In general, any reaction diffusion system can be nondimensionalised and scaled in a similar way, and written in the form:

$$\frac{\partial u}{\partial t} = \gamma f(u,v) + \nabla^2 u \qquad\qquad \frac{\partial v}{\partial t} = \gamma g(u,v) + d\nabla^2 v\,,$$

where $f(u,v)$ and $g(u,v)$ are nonlinear functions, representing the reaction kinetics of the system, and d is the ratio of the diffusion coefficients.

1.2 General conditions for Turing instability

1.2.1 Mathematical formulation of the problem

The equations that describe the system we want to study are therefore the following:

$$\frac{\partial u}{\partial t} = \gamma\left(a - bu + c\frac{u^2}{v}\right) + \nabla^2 u \qquad\qquad \frac{\partial v}{\partial t} = \gamma(u^2 - v) + d\nabla^2 v \quad .$$

In order to formulate correctly the problem from a mathematical point of view, we must establish where u and v are defined and which are the initial and boundary conditions.
Let us call $\mathfrak{D}$ the domain within which the reagents diffuse and react, so that in general u and v will be functions of $\vec{r}$ and t with $\vec{r} \in \mathfrak{D}$.
As for the initial conditions, we take them to be a random perturbation about the homogeneous steady state of the system.
The boundary conditions we consider are:

$$\begin{cases} \vec{n} \cdot \nabla u(\vec{r},t) = 0 \\ \vec{n} \cdot \nabla v(\vec{r},t) = 0 \end{cases} \qquad \vec{r} \in \partial\mathfrak{D}$$

where $\vec{n}$ is the unit outward normal to the boundary of the domain $\partial\mathfrak{D}$. These are zero flux boundary conditions (i.e. a particular case of von Neumann conditions), and we have imposed them because we are interested in self-organizing pattern formation. In fact, the requirement of no flux through $\partial\mathfrak{D}$ is equivalent to have no external input, which can influence the dynamic of patterning.

Summarizing, we have:

$$\frac{\partial u}{\partial t} = \gamma\left(a - bu + c\frac{u^2}{v}\right) + \nabla^2 u \qquad \frac{\partial v}{\partial t} = \gamma(u^2 - v) + d\nabla^2 v \tag{1.2.1}$$

$$\text{with } u(\vec{r},0) \text{ and } v(\vec{r},0) \text{ given} \qquad \text{and} \qquad \begin{cases} \vec{n}\cdot\nabla u(\vec{r},t) = 0 \\ \vec{n}\cdot\nabla v(\vec{r},t) = 0 \end{cases} \qquad \vec{r}\in\partial\mathfrak{D} \quad .$$

Since we are interested in studying the conditions under which the system shows Turing instability, we are going to determine when the homogeneous steady state of the system is linearly stable, and then when the steady state itself is unstable in presence of diffusion.

1.2.2 Linear stability of the homogeneous steady state

The homogeneous steady state (u_0, v_0) of the system is given by:

$$\begin{cases} f(u,v) = 0 \\ g(u,v) = 0 \end{cases} \qquad \Rightarrow \qquad u_0 = \frac{a+c}{b} \qquad v_0 = u_0^2 = \left(\frac{a+c}{b}\right)^2$$

By setting $\vec{w} = \binom{u-u_0}{v-v_0}$ and linearising about the steady state $\vec{w} = 0$, we have:

$$\frac{\partial \vec{w}}{\partial t} = \gamma A \vec{w} \qquad \text{with} \quad A = \begin{pmatrix} f_u & f_v \\ g_u & g_v \end{pmatrix} \tag{1.2.2}$$

where:

$$f_u \equiv \frac{\partial f}{\partial u}_{|(u_0,v_0)} = b\frac{c-a}{c+a} \qquad f_v \equiv \frac{\partial f}{\partial v}_{|(u_0,v_0)} = -\frac{b^2 c}{(a+c)^2}$$

$$g_u \equiv \frac{\partial g}{\partial u}_{|(u_0,v_0)} = 2\frac{a+c}{b} \qquad g_v \equiv \frac{\partial g}{\partial v}_{|(u_0,v_0)} = -1$$

We now look for solutions of (1.2.2) in the form $\vec{w} \propto e^{\lambda t}$: this gives the condition $\det(\lambda \mathbb{1} - \gamma A) = 0$, which means that λ is eigenvalue of γA.
The steady state will be linearly stable if $\mathrm{Re}\,\lambda < 0$, which occurs if:

$$\mathrm{tr}\, A = f_u + g_v < 0 \qquad \Rightarrow \qquad b\frac{c-a}{c+a} < 1 \tag{1.2.3}$$

$$\det A = f_u g_v - f_v g_u > 0 \qquad \Rightarrow \qquad b > 0 \tag{1.2.4}$$

1.2.3 Linear instability of the steady state with diffusion

We now linearise about the same steady state the full equations, getting:

$$\frac{\partial \vec{w}}{\partial t} = \gamma A\vec{w} + D\nabla^2\vec{w} \qquad\qquad D = \begin{pmatrix} 1 & 0 \\ 0 & d \end{pmatrix} \tag{1.2.5}$$

To solve this system, we call $\vec{W}_k$ the time-independent solution of the eigenvalue problem:

$$\nabla^2\vec{W}_k + k^2\vec{W}_k = 0 \qquad\qquad (\vec{n}\cdot\nabla)\vec{W}_k(\vec{r}) = 0 \quad \text{with } \vec{r}\in\partial\mathfrak{D} \tag{1.2.6}$$

relative to the eigenvalue k^2, and then look for solutions $\vec{w}(\vec{r},t)$ of (1.2.5) in the form:

$$\vec{w}(\vec{r},t) = \sum_k c_k e^{\lambda t}\vec{W}_k(\vec{r}) \tag{1.2.7}$$

where λ is the eigenvalue that determines the temporal growth, and c_k are constants that can be determined with an expansion of the initial conditions in terms of $\vec{W}_k$. By substituting (1.2.7) in (1.2.5), and taking advantage of the linearity of the equations, we get:

$$\det(\lambda\mathbb{1} - \gamma A + Dk^2) = 0 \quad \Rightarrow \quad \lambda^2 + \lambda[k^2(1+d) - \gamma(f_u + g_v)] + h(k^2) = 0 \tag{1.2.8}$$

where:

$$h(k^2) = dk^4 - \gamma(df_u + g_v)k^2 + \gamma^2 \det A\,. \tag{1.2.9}$$

For the Gierer and Meinhardt's system, equations (1.2.8) and (1.2.9) become:

$$\lambda^2 + \lambda\left[k^2(1+d) - \gamma\left(b\frac{c-a}{c+a} - 1\right)\right] + h(k^2) = 0 \tag{1.2.10}$$

and:

$$h(k^2) = dk^4 - \gamma\left(db\frac{c-a}{c+a} - 1\right)k^2 + \gamma^2 b\,.$$

Therefore, the steady state will be unstable to spatial perturbations if $\operatorname{Re}\lambda(k^2) > 0$ for some $k \neq 0$. This happens if either the coefficient of λ in (1.2.8) is negative or if $h(k^2) < 0$ for some nonzero k. However, because of condition (1.2.3) and the fact that k^2, d and γ are positive, the coefficient of λ is always positive and thus the only way for $\operatorname{Re}\lambda$ to be positive is when $h(k^2) < 0$ for some $k \neq 0$. Since $\det A = b > 0$ from (1.2.9), one gets $df_u + g_v > 0$, namely:

$$db\frac{c-a}{c+a} > 1 \tag{1.2.11}$$

This, together with (1.2.3), implies that $d > 1$, and that f_u and g_v must have opposite signs. Since $g_v = -1 < 0$, we must have:

$$\frac{c-a}{c+a} > 0 \qquad \Rightarrow \qquad \begin{cases} c > a \\ c < -a \end{cases} \quad \text{if } a > 0 \qquad \begin{cases} c > -a \\ c < a \end{cases} \quad \text{if } a < 0$$

or equivalently:

$$-c < a < c \quad \text{if} \quad c > 0 \qquad\qquad c < a < -c \quad \text{if} \quad c < 0$$

depending whether we consider a or c fixed.
However, by definition a and c must be positive, and so these conditions become:

$$c > a\,. \tag{1.2.12}$$

Inequality (1.2.11) is a necessary but not sufficient condition for $h(k^2)$ to be negative for some nonzero k. Since from (1.2.9) we see that $h(k^2)$ is a parabola in k^2 opening upward, this condition will be satisfied if the minimum $h_{\min}$ is negative, namely:

$$k^2_{\min} = \gamma \frac{df_u + g_v}{2d} = \frac{\gamma}{2d}\left(db\frac{c-a}{c+a} - 1\right),$$

$$h_{\min} = h(k^2_{\min}) = \gamma^2\left[\det A - \frac{(df_u + g_v)^2}{4d}\right] < 0 \qquad \Rightarrow \qquad \frac{(df_u + g_v)^2}{4d} > \det A$$

which, for Gierer and Menihardt's equations, becomes:

$$\left(db\frac{c-a}{c+a} - 1\right)^2 > 4db\,.$$

Therefore, the conditions under which Gierer and Meinhardt's system exhibits Turing instability are:

$$b\frac{c-a}{c+a} < 1\,, \qquad b > 0\,, \qquad db\frac{c-a}{c+a} > 1\,, \qquad \left(db\frac{c-a}{c+a} - 1\right)^2 > 4db\,. \tag{1.2.13}$$

If these inequalities are satisfied, there is a range of k^2 within which $h(k^2)$ is negative, and therefore from (1.2.10) we can see that $\operatorname{Re}\lambda(k^2) > 0$ in the very same range. In particular, this will happen for k^2 within the zeros of $h(k^2)$, namely:

$$k^2_- < k^2 < k^2_+ \qquad k^2_\pm = \frac{\gamma}{2d}\left[\left(db\frac{c-a}{c+a} - 1\right) \pm \sqrt{\left(db\frac{c-a}{c+a} - 1\right)^2 - 4db}\right]. \tag{1.2.14}$$

Thus, all the modes within this range will be unstable and initially grow exponentially with time. Considering the solution $\vec{w}$ of (1.2.5), this means that the relevant contributions to $\vec{w}$ as t increases are these unstable modes, since all the other ones have $\mathrm{Re}\,\lambda < 0$ and then decay with time.
Therefore, for t large enough we have:

$$\vec{w}(\vec{r},t) \approx \sum_{k_1}^{k_2} c_k e^{\lambda(k^2)t}\vec{W}_k(\vec{r})\,, \tag{1.2.15}$$

where k_1 is the smallest eigenvalue greater or equal to k_- and k_2 is the largest eigenvalue lower or equal to k_+, in the case of finite domains (and therefore discrete possible values of k). We can therefore expect that the modes within (1.2.14) will be the ones that determine the emerging pattern.
We must however note that $\mathrm{Re}\,\lambda(k^2)$ has a maximum for $k^2 = k^2_{\min}$, and therefore there will be one fastest growing mode, which will generally be the one that mostly influences the final pattern. Furthermore, we must remember that (1.2.15) is the solution of the linearised system, and therefore if it was valid for all time we would have $\lim_{t\to\infty}\vec{w} = \infty$; this doesn't occur with the solution of the complete nonlinear system, since in this case the nonlinear reaction terms will become relevant for great t, and limit the growth of $\vec{w}$ until a final steady state is reached.

The results that we have just determined are completely general, since we have never used any particular hypothesis concerning the domain $\mathfrak{D}$ of the system (except for the boundary conditions, which are needed for the mathematical well-posedness of the problem and do not affect the validity of what we have found).
In other words, the possibility for a system to exhibit diffusion-driven instability depends only on the chemical properties of the reagents involved, and not on the scale or geometry of the system itself.

Therefore, regardless of the shape and dimension of $\mathfrak{D}$, the conditions that a system must satisfy in order to exhibit Turing instability are given by (1.2.13).

1.3 Turing space

Conditions (1.2.13) on the parameters a, b, c and d in (a,b,c,d) space define a parameter domain, called *Turing space*, within which the system will exhibit diffusion-driven instability. However, even if the parameters of the system lie within Turing space, this doesn't necessarily mean that the system will indeed develop a spatial pattern: in fact, we must also have γ large enough so that at least one possible unstable mode exists. We will later cover this topic in more detail.

1.3.1 Determination of Turing space

The domain defined by inequalities (1.2.13) is not straightforward to represent (also because it lives in a four-dimensional space); we are therefore going to introduce some simplifications in order to make the problem easier to study, and then generalise as much as we can.
Let us then consider c and d fixed, so that we can first determine two-dimensional sections of Turing space in (a, b) space.

In order to determine an explicit representation of this domain we use Murray's method (see [5]), i.e. we set u_0 as a non-negative parametric variable and express v_0 and b in terms of u_0 and a. We thus have:

$$v_0 = u_0^2\,, \qquad\qquad b = \frac{a+c}{u_0}$$

and:

$$f_u = \frac{c-a}{u_0}\,, \qquad f_v = -\frac{c}{u_0^2}\,, \qquad g_u = 2u_0\,, \qquad g_v = -1\,.$$

We now express the conditions for Turing instability in terms of u_0, so that we can determine regions of (a, b) plane enclosed by parametric curves.
The Turing space of the system will then be given by the intersection of these regions.

We therefore have:

$$f_u + g_v < 0 \quad \Rightarrow \quad a > c - u_0 \qquad b > \frac{2c}{u_0} - 1 \tag{1.3.1a}$$

$$f_u g_v - f_v g_u > 0 \quad \Rightarrow \quad a > -c \qquad b > 0 \tag{1.3.1b}$$

$$df_u + g_v > 0 \quad \Rightarrow \quad a < c - \frac{u_0}{d} \qquad b < \frac{2c}{u_0} - \frac{1}{d} \tag{1.3.1c}$$

As of the last condition, $(df_u + g_v)^2 - 4d(f_u g_v - f_v g_u) > 0$ brings to:

$$a < -2\sqrt{\frac{2c}{d}u_0} + c + \frac{u_0}{d} \qquad b < -2\sqrt{\frac{2c}{u_0 d}} + \frac{2c}{u_0} + \frac{1}{d} \tag{1.3.1d}$$

$$a > 2\sqrt{\frac{2c}{d}u_0} + c + \frac{u_0}{d} \qquad b > 2\sqrt{\frac{2c}{u_0 d}} + \frac{2c}{u_0} + \frac{1}{d} \tag{1.3.1e}$$

We can now see that some of these inequalities are redundant; for example, (1.3.1b) is automatically satisfied by conditions (1.2.12) and (1.2.4). Furthermore, if we impose (1.3.1d) then (1.3.1c) is certainly valid; in fact, we have:

$$-2\sqrt{\frac{2c}{d}u_0} + c + \frac{u_0}{d} < c - \frac{u_0}{d} \qquad \Leftrightarrow \qquad u_0 < 2cd$$

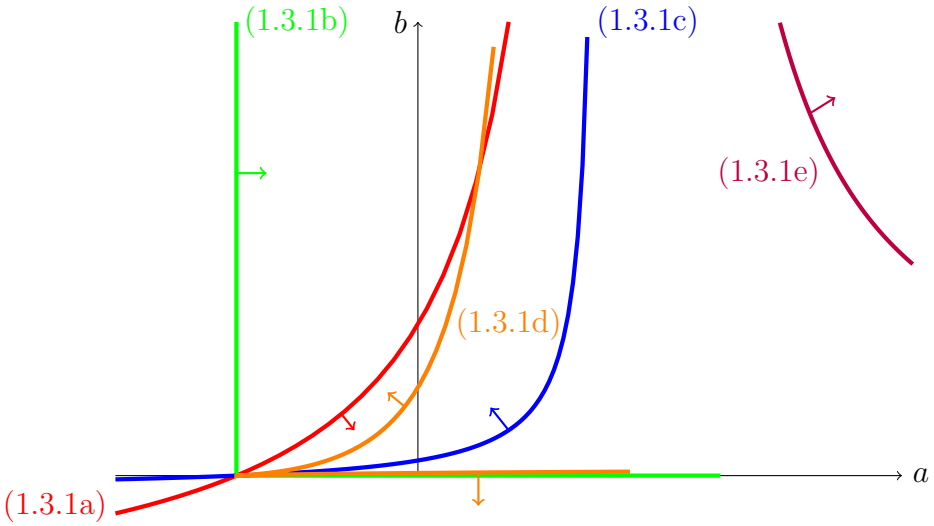

Figure 1.1: Graphical representation of (1.3.1a)-(1.3.1e). The arrows show the parts of (a, b) plane defined by those inequalities. The Turing space of the system is given by their intersection, which is the region between (1.3.1a) and (1.3.1d).

and for $u_0 = 2cd$, the parametric curve that defines (1.3.1d) has $a = -c$ and $b = 0$, which is the point where it intersects (1.3.1a) and (1.3.1c). Finally, we see that (1.3.1e) cannot be valid if either (1.3.1a) or (1.3.1c) are satisfied: this happens because the last condition for Turing instability determines two distinct and not connected regions of (a, b) space (i.e. inequalities (1.3.1d) and (1.3.1e)), and the intersection of (1.3.1a) and (1.3.1c) with (1.3.1e) is empty, while that with (1.3.1d) is not.
Furthermore, we must also remember to impose conditions $a > 0$ and $c > 0$, since a and c are positive by definition.

Everything becomes clearer if we plot together the regions of (a, b) space given by (1.3.1a)-(1.3.1e) (see figure 1.1).

We must remember that a and c are positive, and so we must also impose the supplementary conditions $a > 0$ and $c > 0$.

We can therefore see that for such a system a critical value for d exists: in fact, we can first note that when $d < 1$ inequalities (1.3.1a) and (1.3.1c) contradict each other, and so we surely must have $d > 1$ for a possible Turing space to exist. However, this is not a sufficient condition: as we can deduce from figure 1.1, it can be possible that the solution of inequalities (1.3.1a)-(1.3.1e) (i.e. the intersection of the regions of (a, b) space determined by (1.3.1a) and (1.3.1d)) lies in the region

$a < 0$, and so in these conditions no actual Turing space exists.
Therefore, in order to find the critical value d_c for d we determine the intersection of the parametric curves (1.3.1a) and (1.3.1d), setting:

$$c - u_0 = -2\sqrt{\frac{2c}{d}u_0} + c + \frac{u_0}{d} \qquad \Rightarrow \qquad u_0 = 8c\frac{d}{(d+1)^2}\,.$$

Thus, the value of a where (1.3.1a) and (1.3.1d) intersect each other is:

$$a = c - u_0 = c\left[1 - 8\frac{d}{(d+1)^2}\right]\,.$$

By setting $a > 0$, we get:

$$d^2 - 6d + 1 > 0\,,$$

whose solution is $d < 3-2\sqrt{2}$ or $d > 3+2\sqrt{2}$. However, since d must be greater than 1, for what stated previously, the only valid solution of the inequality is $d > 3+2\sqrt{2}$. Therefore, $d_c = 3 + 2\sqrt{2}$ and if $d < d_c$ (with all the other parameters kept fixed) no Turing space exists.

1.3.2 Representation of Turing space

Therefore, Turing space for Gierer and Menihardt's system is, for c and d fixed, the region of (a, b) space enclosed between the two parametric curves:

$$(1.3.1a): \begin{cases} a = c - u_0 \\ b = \frac{2c}{u_0} - 1 \end{cases} \qquad (1.3.1d): \begin{cases} a = -2\sqrt{\frac{2c}{d}u_0} + c + \frac{u_0}{d} \\ b = -2\sqrt{\frac{2c}{u_0 d}} + \frac{2c}{u_0} + \frac{1}{d} \end{cases}$$

with $a, c > 0$.
Figure 1.2 represents some examples of two-dimensional sections of Turing space for various values of fixed c and d, while in figure 1.3 Turing space is represented in (a, b, c) space, for d fixed.

1.3.3 Notes on Turing space

We can now deduce some general properties of Gierer and Meinhardt's system.

From figure 1.3, we can see that it is not very *robust*: since its Turing space is quite "narrow", reaction-diffusion systems obeying Gierer and Meinhardt's equations can be very sensible to random perturbations, which are always present in biological contexts.

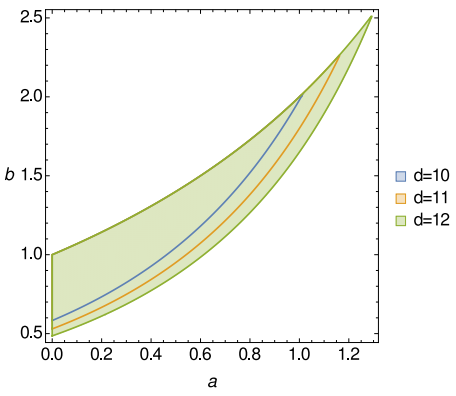

(a) $c = 3$

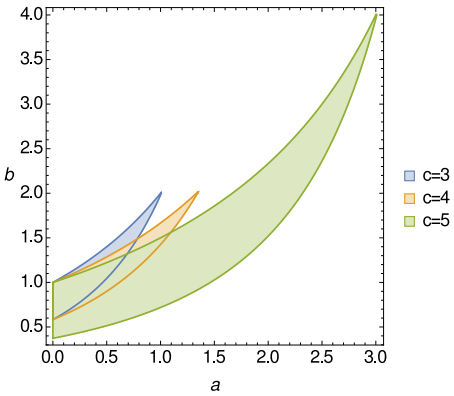

(b) $d = 10$

Figure 1.2: Two-dimensional sections of Turing space for some values of c and d.

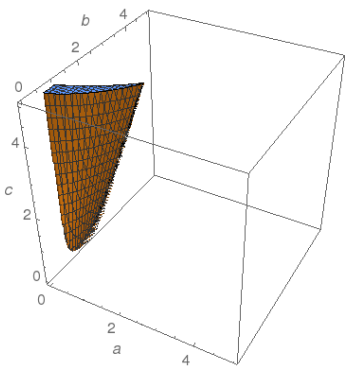

(a) $d = 10$

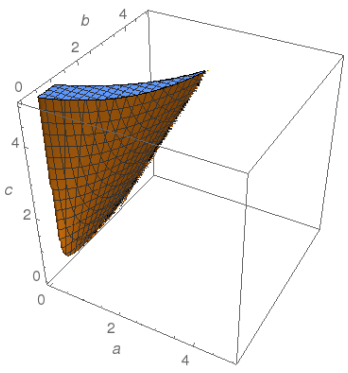

(b) $d = 15$

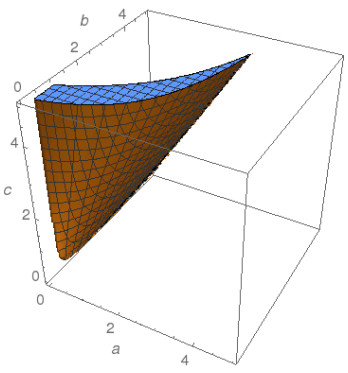

(c) $d = 20$

Figure 1.3: Representation of Turing space for various values of d.

We can also note that diffusion-driven instability is the result of a combination of various effects: if we suppose the system to be initially outside Turing space, then there will be several ways by which we can make it diffusively unstable; in fact, by varying one or more of the parameters of the system we can "move" it inside Turing space, and there is no single way to do it. Therefore, there will be different and equivalent effects, through the variation of the parameters of the system, that will lead to the formation of the same patterns.

Chapter 2

Gierer and Meinhardt's system on a sphere

We will now proceed to the main part of this work, namely the study of Gierer and Meinhardt's system defined on a sphere of radius R, in order to investigate the effects of curvature on pattern formation.

2.1 Initial considerations

The mathematical formulation of the problem we want to analyse is the following:

$$\frac{\partial u}{\partial t} = \gamma\left(a - bu + c\frac{u^2}{v}\right) + \nabla^2 u \qquad \frac{\partial v}{\partial t} = \gamma(u^2 - v) + d\nabla^2 v$$

$$u(\theta, \varphi, 0) \text{ and } v(\theta, \varphi, 0) \text{ given,}$$

where we have written u and v in spherical coordinates, since $\mathfrak{D}$ is now a sphere of (fixed) radius R, and curvature $\rho = 1/R$. Since the problem is defined on a sphere, no boundary conditions are required.

Note that γ is related to the curvature of the sphere, namely its size. By taking R as a characteristic length of the system we have $\gamma = R^2 k_5/D_A = (1/\rho^2)(k_5/D_A)$. We therefore must keep in mind that $\gamma \propto R^2 = 1/\rho^2$, since this will be important to determine the effects of curvature on spatial pattern formation on a sphere. For future convenience, we set $\gamma = \Gamma/\rho^2$ (namely, $\Gamma = k_5/D_A$).

The eigenvalue problem we have to solve now is:

$$\nabla^2 \vec{W}_k + k^2 \vec{W}_k = 0 \qquad \vec{W}_k \text{ defined on } \mathfrak{D}\,,$$

whose solutions are the spherical harmonics $Y_\ell^m(\theta,\varphi)$. Therefore we have:

$$k^2 = \frac{\ell(\ell+1)}{R^2} = \rho^2\ell(\ell+1) \tag{2.1.1}$$

(where $\ell = 0, 1, 2, \dots$) and we look for solutions of the complete linearised system in the form:

$$\vec{w}(\theta,\varphi,t) = \sum_{\ell=0}^{\infty}\sum_{m=-\ell}^{\ell} \vec{C}_\ell^m e^{\lambda t} Y_\ell^m(\theta,\varphi)\,, \tag{2.1.2}$$

where $\vec{C}_\ell^m$ are constants determined with an expansion of the initial conditions in terms of spherical harmonics.

We can now apply all the results we have determined in 1.2 with the substitution (2.1.1), which is the particular form of the eigenvalues of the Laplacian in this case. We thus have:

$$k^2_{\min} = \rho^2\ell_{\min}(\ell_{\min}+1) = \frac{\hat{\Gamma}}{2d\rho^2}\,,$$

where we have set, for the sake of convenience, $\hat{\Gamma} = \Gamma\left(db\frac{c-a}{c+a} - 1\right)$. Therefore:

$$\ell^2_{\min} + \ell_{\min} - \frac{\hat{\Gamma}}{2d\rho^4} = 0 \qquad \Rightarrow \qquad \ell_{\min} = -\frac{1}{2} + \frac{1}{2}\sqrt{1 + \frac{2\hat{\Gamma}}{d\rho^4}}$$

and:

$$h(\ell_{\min}) = \frac{1}{\rho^4}\left(\Gamma^2 b - \frac{\hat{\Gamma}^2}{4d}\right)\,. \tag{2.1.3}$$

The range of unstable modes is then given by:

$$\ell_- < \ell < \ell_+\,, \qquad \ell_\pm = -\frac{1}{2} + \frac{1}{2}\sqrt{1 + \frac{2}{d\rho^4}\left(\hat{\Gamma} \pm \sqrt{\hat{\Gamma}^2 - 4db\Gamma^2}\right)}\quad. \tag{2.1.4}$$

Of course, this could also be determined by explicitly substitute (2.1.2) in system (1.2.5). In fact, by proceeding like in section 1.2.3 we find:

$$\lambda^2 + \lambda\left[\rho^2\ell(\ell+1)(1+d) - \frac{\Gamma}{\rho^2}\left(b\frac{c-a}{c+a} - 1\right)\right] + h(\ell) = 0\,, \tag{2.1.5}$$

$$h(\ell) = d\rho^4\ell^4 + 2d\rho^4\ell^3 + (d\rho^4 - \hat{\Gamma})\ell^2 - \hat{\Gamma}\ell + \frac{\Gamma^2}{\rho^4}b\,. \tag{2.1.6}$$

The behaviour of $h(\ell)$ is reported in figure 2.1. Note that $h(\ell)$ has only one minimum for $\ell > 0$. In fact:

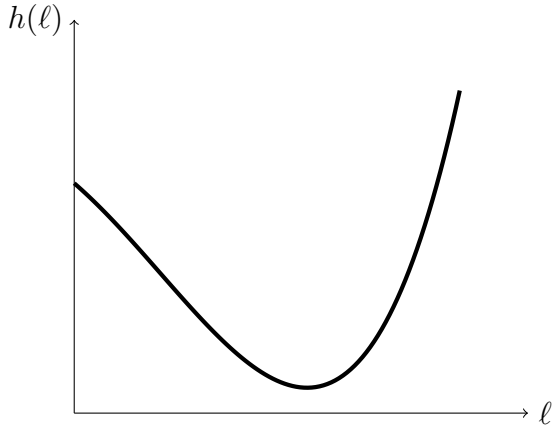

Figure 2.1: General trend of $h(\ell)$

$$\begin{aligned} h'(\ell) &= 4d\rho^4\ell^3 + 6d\rho^4\ell^2 + 2(d\rho^4 - \hat{\Gamma})\ell - \hat{\Gamma} \\ &= (2\ell+1)(2d\rho^4\ell^2 + 2\rho^4\ell - \hat{\Gamma}) \end{aligned}$$

and so $h'(\ell) = 0$ if:

$$\ell = \ell_0 = -\frac{1}{2} \qquad \text{or} \qquad \ell = \ell_{2,1} = -\frac{1}{2} \pm \frac{1}{2}\sqrt{1 + \frac{2\hat{\Gamma}}{d\rho^4}}\,.$$

Among these, ℓ_2 is the only positive root of $h(\ell)$, and we see that $\ell_2 = \ell_{\min}$.
We can also note that by substituting $\ell_{\min}$ in (2.1.6) we get exactly (2.1.3), and that the condition $h(\ell_{\min}) < 0$ gives:

$$\left(db\frac{c-a}{c+a} - 1\right)^2 > 4db\,,$$

which is the last condition for Turing instability; this is exactly what happened in the general case discussed in section 1.2, as we expected.
It can also be shown by substitution in (2.1.4) that $\ell_\pm$ are indeed the two positive roots of $h(\ell)$.

From (2.1.6) we see that $h(0) = \Gamma^2 b/\rho^4 > 0$ for any choice of the parameters of the system (within Turing space, of course). This remarkable property means that the mode with $\ell = 0$ will *never* become unstable; this is coherent with the fact that Y_0^0 is a constant function, and the system will never evolve into a homogeneous state.

2.2 The role of curvature

If the parameters of the system lie within the Turing space, there will always be an interval of unstable modes, given by (2.1.4).
However, even if there is a range of ℓ such that $h(\ell) < 0$, this does not necessarily mean that the system will indeed develop spatial patterns: in fact, the possible values of ℓ are discrete, and so we must have at least one of them within the range $\ell_- < \ell < \ell_+$ for a spatial pattern to develop.

2.2.1 The effects of curvature

In order to investigate how curvature affects the possible available unstable modes, we will now study how $h(\ell)$ varies as a function of ρ when all other parameters are kept fixed.

By considering the expression of $\ell_{\min}$:

$$\ell_{\min} = -\frac{1}{2} + \frac{1}{2}\sqrt{1 + \frac{2\hat{\Gamma}}{d\rho^4}} \qquad \Rightarrow \qquad \lim_{\rho\to 0} \ell_{\min} = +\infty \qquad \lim_{\rho\to\infty} \ell_{\min} = 0^+$$

and, for $h(\ell_{\min})$, we have (remembering that $\Gamma^2 b - \hat{\Gamma}^2/4d < 0$ within Turing space):

$$h(\ell_{\min}) = \frac{1}{\rho^4}\left(\Gamma^2 b - \frac{\hat{\Gamma}^2}{4d}\right) \qquad \Rightarrow \qquad \lim_{\rho\to 0} h(\ell_{\min}) = -\infty \qquad \lim_{\rho\to\infty} h(\ell_{\min}) = 0^-\,,$$

while, for $h(0)$:

$$h(0) = \frac{\Gamma^2}{\rho^4} b \qquad \Rightarrow \qquad \lim_{\rho\to 0} h(0) = +\infty \qquad \lim_{\rho\to\infty} h(0) = 0^+\,.$$

It is interesting to see how the width of the range of unstable modes changes with ρ. We have:

$$\ell_+ - \ell_- = \frac{1}{2}\left(\sqrt{1 + \frac{\alpha}{\rho^4}} - \sqrt{1 + \frac{\beta}{\rho^4}}\right)$$

where:

$$\alpha = \frac{2}{d}\left(\hat{\Gamma} + \sqrt{\hat{\Gamma}^2 - 4db\Gamma^2}\right) \qquad \beta = \frac{2}{d}\left(\hat{\Gamma} - \sqrt{\hat{\Gamma}^2 - 4db\Gamma^2}\right)\,,$$

and thus $\alpha > \beta$.
When $\rho \sim \infty$, $1/\rho^4 \sim 0$ and so with a Taylor series expansion in terms of $1/\rho^4$ we have:

$$\ell_+ - \ell_- \overset{\rho\sim\infty}{\sim} \frac{1}{2}\left(1 + \frac{\alpha}{2}\frac{1}{\rho^4} - 1 - \frac{\beta}{2}\frac{1}{\rho^4}\right) = \frac{\alpha - \beta}{4}\frac{1}{\rho^4}\,,$$

giving:

$$\lim_{\rho\to\infty} \ell_+ - \ell_- = 0^+ .$$

In order to analyse the trend of $\ell_+ - \ell_-$ when $\rho \sim 0$, it is more convenient to perform a Laurent series expansion. In particular, if we call:

$$f(\rho) = \sqrt{1 + \frac{C}{\rho^4}} = \frac{\sqrt{\rho^4 + C}}{\rho^2}$$

where C is a real constant, we see that $f(\rho)$ has a pole of order two at $\rho = 0$. Writing the Laurent series of f as:

$$f(\rho) = \sum_{k=-2}^{\infty} d_k \rho^k , \qquad d_k = \frac{1}{2\pi i} \oint_{\mathcal{C}} \frac{1}{\rho^{k+1}} f(\rho) d\rho = \text{Res} \left\{ \frac{\sqrt{\rho^4 + C}}{\rho^{k+3}} \right\}_{\rho=0} ,$$

(where $\mathcal{C}$ is a counterclockwise circle enclosing $\rho = 0$), we have:

$$d_{-2} = \text{Res} \left\{ \frac{\sqrt{\rho^4 + C}}{\rho} \right\}_{\rho=0} = \lim_{\rho\to 0} \sqrt{\rho^4 + C} = \sqrt{C} .$$

Therefore:

$$\ell_+ - \ell_- \overset{\rho\sim 0}{\sim} \frac{1}{2} \left(\frac{\sqrt{\alpha}}{\rho^2} - \frac{\sqrt{\beta}}{\rho^2} \right) = \frac{\sqrt{\alpha} - \sqrt{\beta}}{2} \frac{1}{\rho^2} \qquad \Rightarrow \qquad \lim_{\rho\to 0} \ell_+ - \ell_- = +\infty .$$

Summarizing:

$$\lim_{\rho\to 0} \ell_{\min} = +\infty \qquad \lim_{\rho\to\infty} \ell_{\min} = 0^+ \qquad \lim_{\rho\to 0} h(\ell_{\min}) = -\infty \qquad \lim_{\rho\to\infty} h(\ell_{\min}) = 0^-$$

$$\lim_{\rho\to 0} h(0) = +\infty \qquad \lim_{\rho\to\infty} h(0) = 0^+ \qquad \lim_{\rho\to 0} (\ell_+ - \ell_-) = +\infty \qquad \lim_{\rho\to\infty} (\ell_+ - \ell_-) = 0^+$$

The behaviour of $h(\ell)$ for different values of ρ is represented in figure 2.2.

If the sphere is very small, i.e. if its curvature is very large, $h(\ell)$ will be "squeezed" towards the vertical axis, and therefore no spatial pattern will form since none of the possible ℓ will lie within the range $\ell_- < \ell < \ell_+$. If we now choose a sphere of larger radius, the range of unstable modes will move along the ℓ axis and become wider: at a certain point the lowest possible eigenvalue, i.e. $\ell = 1$, will fall within the range and thus become unstable. This will happen when:

$$\ell_+ = 1 \qquad \Rightarrow \qquad \rho = \rho_{\text{crit}} = \left[\frac{1}{4d} \left(\hat{\Gamma} + \sqrt{\hat{\Gamma}^2 - 4db\Gamma^2} \right) \right]^{1/4} .$$

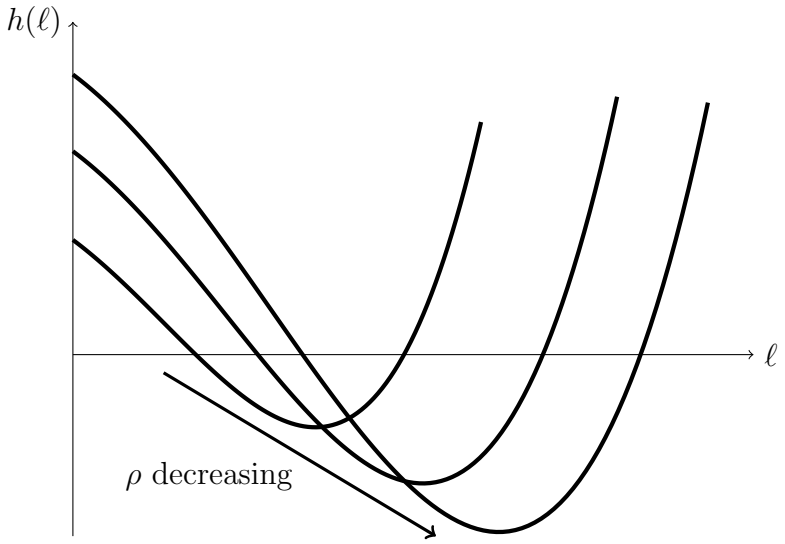

Figure 2.2: Plots of $h(\ell)$ for various values of ρ

We can therefore understand the first important role of curvature in pattern formation: the existence of a *critical curvature*, namely a critical size for the sphere above which patterning can occur. In other words if the sphere is too small ($\rho > \rho_{\text{crit}}$) the system will *never* be able to develop inhomogeneous spatial patterns, even if it satisfies the conditions for diffusion-driven instability.

Let us now further decrease the curvature of the sphere: the band of unstable modes will widen and include more and more possible unstable modes, while the minimum of $h(\ell)$ will become more and more negative. This means that as the size of the sphere increases, the fastest growing mode (i.e. the one relative to the eigenvalue nearest to ℓ_{min}) becomes more and more relevant, and so we can expect that it will be the dominant term of the solution of the linearised system, i.e. the mode that determines the final pattern. In fact, if an unstable modes grows sufficiently fast it will quickly dominate and survive through the nonlinear region.

Actually, this happens only for the lower modes: numerical simulations (see [9]) have shown that for the higher ones the effects of the nonlinearities of the equations on the evolution of the system become more complex than when only the lower modes are unstable, leading to patterns that can be considerably different from those predicted by linear analysis. In general, we have that linear analysis leads to reliable predictions only for low modes, and it can be shown with singular perturbation analyses that this still holds true in near-bifurcation conditions. However,

we must note that this method determines correctly parameter ranges for pattern formation, namely Turing space.

Therefore, for big enough spheres the final steady state can be different from what we can predict with the method we are using.

2.2.2 Mode selection

We would now like to answer a simple question: how can we excite a selected mode? In other words, by changing the radius of the sphere, how can we make sure that a given mode will become unstable and hence determine the final pattern?
We can use what we have previously stated so that the selected mode will have the largest growth factor. If we call ℓ_{chs} the eigenvalue of the mode we have chosen to excite, this will occur if $\ell_{\text{min}} = \ell_{\text{chs}}$, namely:

$$\rho = \left\{ \frac{2\hat{\Gamma}}{d\left[(2\ell_{\text{chs}}+1)^2 - 1\right]} \right\}^{1/4} .$$

2.3 The role of initial conditions

Until now we have always neglected the effects that initial conditions might have on the evolution of spatial patterns. As we shall now see, they are extremely important and determine some relevant properties of the final pattern.

2.3.1 Polarity

We have seen in section 1.2.3 that in general if a system is diffusively unstable and a range of possible unstable modes exists, for t large enough the solution $\vec{w}$ of the complete linearised system of Gierer and Meinhardt's equations is (1.2.5):

$$\vec{w}(\vec{r},t) \approx \sum_{k_1}^{k_2} c_k e^{\lambda(k^2)t} \vec{W}_k(\vec{r})$$

where k_1 and k_2 are, respectively, the smallest and largest possible eigenvalues within the range of unstable modes.
In the case we are considering, i.e. when the domain $\mathfrak{D}$ is a spherical surface, we have:

$$\vec{w}(\theta,\varphi,t) \approx \sum_{\ell=\ell_1}^{\ell_2} \sum_{m=-\ell}^{\ell} \vec{C}_\ell^m e^{\lambda(\ell)t} Y_\ell^m(\theta,\varphi) \tag{2.3.1}$$

where ℓ_1 is the smallest eigenvalue greater or equal to ℓ_- and ℓ_2 is the largest one lower or equal to ℓ_+.
Let us now suppose, for example, that the system is such that only the mode with $\ell = 1$ and $m = 0$ is unstable; we then have:

$$\vec{w}(\theta, \varphi, t) \approx \vec{C}_1^0 e^{\lambda(1)t} Y_1^0(\theta, \varphi)$$

and $\vec{C}_1^0$ is a vector of constants determined, as usual, with an expansion of initial conditions in terms of Y_1^0.
To get a better understanding of how initial conditions can influence the polarity of the final pattern, let us suppose $\vec{C}_1^0$ to be $(\varepsilon, \varepsilon)$ for $\varepsilon > 0$ small. Therefore:

$$\vec{w}(\theta, \varphi, t) \approx \begin{pmatrix} \varepsilon \\ \varepsilon \end{pmatrix} e^{\lambda(1)t} Y_1^0(\theta, \varphi)$$

and considering the single components of $\vec{w}$:

$$u(\theta, \varphi, t) \approx u_0 + \varepsilon e^{\lambda(1)t} Y_1^0(\theta, \varphi) \qquad v(\theta, \varphi, t) \approx v_0 + \varepsilon e^{\lambda(1)t} Y_1^0(\theta, \varphi) \quad .$$

We therefore have that both u and v will finally be spatially arranged like the spherical harmonic of order one, i.e. with $u > u_0$ and $v > v_0$ in one of the two hemispheres.
However, if we now suppose to have $\vec{C}_1^0 = (-\varepsilon, \varepsilon)$, then:

$$u(\theta, \varphi, t) \approx u_0 - \varepsilon e^{\lambda(1)t} Y_1^0(\theta, \varphi) \qquad v(\theta, \varphi, t) \approx v_0 - \varepsilon e^{\lambda(1)t} Y_1^0(\theta, \varphi)$$

which is the same arrangement of the preceding case, but with opposite polarity.
Therefore, we can see that for any possible excited mode we have two possible different patterns, each with opposite polarity, that are both solutions of the linearised system of equations.
This poses some conceptual difficulties under a biological point of view, within the context of prepattern theory: in fact, what we have just seen means that if cells differentiate when the concentration of a morphogen exceeds some threshold level, then the differentiated cell pattern is different for each case. However, development is a sequential process, i.e. every stage of the development induces the next one; therefore this means that there must be a bias in the initial conditions towards one of the possible patterns. This is still an open issue, and is exactly what we have stated in the preface: we still don't know the mechanism that links genetic information and the bias on the initial conditions that leads to the final pattern.

2.3.2 Order of the unstable modes

Another fact that we have completely ignored until now is that in this case spherical harmonics are degenerate with respect to the eigenvalue ℓ. In fact, for a fixed value

of ℓ there are $2\ell+1$ different possible spherical harmonics, and we can only excite a certain value of ℓ, i.e. the degree of the spherical harmonics. Therefore, if we use mode selection in order to excite a particular ℓ, we still don't know exactly what will the final heterogeneous pattern look like because we have no way to select any of those $2\ell+1$ possible spherical harmonics by only varying the parameters of the system.
In fact, if we suppose that the only unstable mode is that relative to the eigenvalue ℓ, (2.3.1) becomes:

$$\vec{w}(\theta,\varphi,t) \approx \sum_{m=-\ell}^{\ell} \vec{C}_\ell^m e^{\lambda(\ell)t} Y_\ell^m(\theta,\varphi)$$

and the order of the final pattern is determined by $\vec{C}_\ell^m$. For example, if we take $\ell=3$ and $\vec{C}_3^2=(\varepsilon,\varepsilon)$ for $\varepsilon>0$ small, while $\vec{C}_3^m=0$ for $m\neq 2$, we will have:

$$\vec{w}(\theta,\varphi,t) \approx \begin{pmatrix}\varepsilon\\ \varepsilon\end{pmatrix} e^{\lambda(3)t} Y_3^2(\theta,\varphi)\,.$$

Therefore, the conceptual difficulty we have described in the preceding section becomes even more challenging if we consider that also the order of the excited spherical harmonic depends on a bias on the initial conditions.

2.4 Conclusions

We have made a simple linear analysis of a system composed of two chemical reagents obeying Gierer and Meinhardt's equations on a spherical surface in order to determine the spatial patterns that might develop from such a system. We have seen that Turing instability occurs when conditions:

$$b\frac{c-a}{c+a}<1\,,\qquad b>0\,,\qquad db\frac{c-a}{c+a}>1\,,\qquad \left(db\frac{c-a}{c+a}-1\right)^2>4db$$

are satisfied, which confirms the predictions already known for flat surfaces. In this case, a range of unstable modes always exists and is given by:

$$\ell_-<\ell<\ell_+\,,\qquad \ell_\pm=-\frac{1}{2}+\frac{1}{2}\sqrt{1+\frac{2}{d\rho^4}\left(\hat{\Gamma}\pm\sqrt{\hat{\Gamma}^2-4db\Gamma^2}\right)}\,,$$

where $\Gamma=k_5/D_A$ and $\hat{\Gamma}=\Gamma\left(db\frac{c-a}{c+a}-1\right)$.
We have then seen how this range behaves as a function of the curvature ρ, and have deduced that a critical value for ρ exists, i.e. is the sphere is too small the system

will never be able to develop inhomogeneous spatial patterns, even if it satisfies the aforementioned conditions for diffusion-driven instability. We have also seen that as the curvature decreases, the range of possible unstable modes becomes wider and thus more complex pattern can be generated as the radius of the sphere increases. Therefore, for a fixed value $R = 1/\rho$ of the radius we can conclude that the set of patterns that can develop from the system are the spherical harmonics of degree ℓ included in the aforementioned range. In particular the dominant pattern (i.e. the one with the largest growth factor) will be that with degree ℓ nearest to $\ell_{\min}$, where:

$$\ell_{\min} = -\frac{1}{2} + \frac{1}{2}\sqrt{1 + \frac{2\hat{\Gamma}}{d\rho^4}} \ .$$

We have also stated that linear prediction is reliable only near bifurcation conditions and for the lowest values of ℓ, and must be used only as a guide to understand the final pattern when higher modes are unstable.
Finally, we have also seen that the order m of the unstable spherical harmonics, as well as their polarity, are determined only by initial conditions.

2.5 Numerical simulations

In this last section we show the results of some numerical simulations, performed in order to study how the final spatial pattern changes with the radius of the sphere. The results of the simulations are shown in figure 2.3.

As we can see, the complexity of the final pattern increases with the radius of the sphere. In particular, if the radius is small the final spatial pattern is indeed a spherical harmonic of first order ($\ell = 1$), as we have determined in this work.

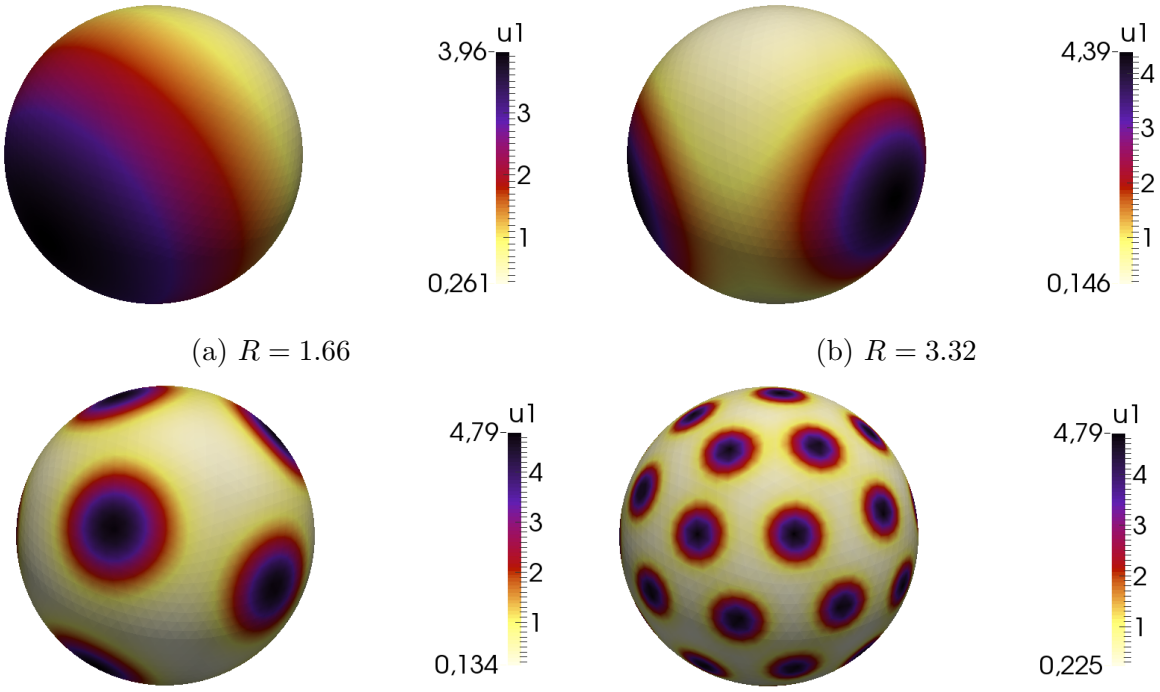

(a) $R = 1.66$ (b) $R = 3.32$

(c) $R = 6.64$ (d) $R = 13.28$

Figure 2.3: Results of the numerical simulations. The sphere has been discretized with a geodetic icosahedral lattice with 2562 points, and initial conditions have been taken, for both u and v, as random distribution within 0 and 1. The evolution of the system has been performed with an Adam-Bashforth-Moluton algorithm, and the derivatives have been computed with finite centred differences. All the simulations have been performed with 10.000.000 time steps, the time of convergence being shorter for smaller radii.
The spatial interval (namely the distance between nearest neighbors) has been taken as approximately 1 for the biggest sphere and then rescaled with the radius; the time interval has been taken as a hundredth of the spatial interval for the biggest sphere, and then rescaled with the square of the radius.

Bibliography

[1] J. D. Murray, *Mathematical Biology (third edition)*, Volume 2, Springer-Verlag, 2003

[2] A. M. Turing, *The chemical basis of morphogenesis*, Philosophical Transactions of the Royal Society of London, series B, 237:37–72, 1952

[3] T. Laux et al., *Genetic regulation of embryonic pattern formation*, The Plant Cell, 2004

[4] A. Gierer and H. Meinhardt, *A theory of biological pattern formation*, Kybernetik, 12:30–39, 1972

[5] J. D. Murray, *Parameter space for Turing instability in reaction diffusion mechanisms: a comparison of models*, Journal of Theoretical Biology, 98:143–163, 1982

[6] A.J. Koch and H. Meinhardt, *Biological pattern formation: from basic mechanisms to complex structures*, Review of Modern Physics, 66:1481–1507, 1994

[7] L. Wolpert, *Positional information and the spatial pattern of cellular differentiation*, Journal of Theoretical Biology, 25:1–47, 1969

[8] G. F. Oster and J. D. Murray, *Pattern formation models and developmental constraints*, The Journal of Experimental Zoology, 251:186–202, 1989

[9] P. Arcuri and J. D. Murray, *Pattern sensitivity to boundary and initial conditions in reaction-diffusion models*, Journal of Mathematical Biology, 24:141–165, 1986